

# MONITORING OF FLUID INJECTION AND SOIL CONSOLIDATION USING SURFACE TILT MEASUREMENTS

By D. W. Vasco,<sup>1</sup> Kenzi Karasaki,<sup>2</sup> and Larry Myer<sup>3</sup>

**ABSTRACT:** Temporal variations of surface tilt may be used for the noninvasive monitoring of subsurface volume change. Such volume changes may accompany settlement near structures, the response due to fluid injection or withdrawal, and excavation-related activity. We outline a methodology for using tilt data to estimate volume changes within poroelastic media. The expressions relating subsurface volume change and surface tilt are simple and compact, offering the possibility of real-time monitoring. The inversion of actual tilt data from a site near Raymond, Calif., generates images of fluid withdrawal from a complex fracture zone about 30 m below the surface. Volume changes are confined to an elongated north-south zone in agreement with independent well test data. We have also applied the methodology for the inversion of surface tilt to data from a grout injection experiment in Los Banos. The technique enables us to monitor grout migration through a porous gravel.

## INTRODUCTION

For many applications, monitoring subsurface fluid flow and volume change is critical. Identifying subsurface volume change is important for monitoring settlement near structures, excavation effects and slope stability. There are numerous economic ventures, such as oil extraction and ground-water utilization, that are aided by the characterization of underground fluid flow. In addition, environmental applications such as ground-water remediation rely on models of contaminant transport in the Earth. Many current techniques for determining subsurface permeability variations, for example, mapping fractures, are very invasive or are only indirectly related to fluid flow. Direct hydrological measurements require numerous wells to adequately estimate flow properties.

Monitoring surface deformation is one noninvasive method for directly inferring volume changes induced by fluid migration and material consolidation. In the last decade, there have been significant advances in our ability to detect changes in the Earth's surface, and there have been an increasing number of applications relating surface deformation to hydrologic processes (Du et al. 1993; Dusseault et al. 1993; Bruno and Nakagawa 1991). It is possible to associate subsurface fluid withdrawal from deep oil wells to surface subsidence (Segall 1985). Currently, several oil field service companies now utilize surface tilt data to monitor hydraulic fracturing (Bruno and Bilak 1994). In addition, vertical displacement measurements have been used to determine fracture geometry and incremental growth associated with waste remediation. Finally, vertical deformation of the Earth's surface has been used to monitor volcanic hazards (Vasco et al. 1988, 1990).

In the present paper, we discuss the use of highly accurate tiltmeter measurements to estimate shallow subsurface fluid movement and consolidation. In particular, we wish to highlight the usefulness of tiltmeter data in mapping the volume change associated with fluid injection or withdrawal. The response of the Earth's surface to a dipping hydro-fracture has been known for some time (Pollard and Holzhausen 1979; Davis 1983). Furthermore, algorithms such as these have been used to infer the geometry of hydro-fractures (Evans et al.

1982; Palmer 1990); however, the degree of opening of the hydro-fracture does not vary spatially over the fracture plane. In the present work, we allow for spatially varying volume changes over a fracture plane, as well as for more general three-dimensional distributions of volume changes. Two applications will be discussed: monitoring fluid withdrawal from a fracture zone in granite and mapping the injection of grout into a shallow gravel deposit.

## Calculating Tilt in Poroelastic Half-Space

Estimation of subsurface volume changes given observations of surface displacement or tilt is a classic inverse problem (Menke 1984). The corresponding forward problem entails calculating the surface response given a model of subsurface volume change. Here, our discussion will be in terms of a small change in subsurface fluid volume. For fluid injection or extraction, this corresponds to material pumped into or out of a well. For consolidation, the volume change would correspond to some amount of pore fluid diffusing or migrating out of a region, resulting in a net loss of pore volume. The material in this section may be related to work on subsidence and consolidation theory (Chilingarian et al. 1995).

The defining equations for the computation of volume change within a porous elastic medium were originally derived for the case of plane strain (Melan 1932; Biot 1941; Rice and Cleary 1976; Segall 1985). Here, we present results for a point volume change in a porous medium for arbitrary strain. Our approach is quasi-static, in that we assume that the transient behavior has decayed for each increment of deformation. In a poroelastic half-space, the important parameters are the solid strains,  $\epsilon_{ij}$ , the stresses,  $\sigma_{ij}$ , and the pore pressure in the fluid,  $p$ . The constitutive equations contain five constants: shear modulus of the solid,  $\mu$ ; Poisson's ratio of the solid,  $\nu$ ; Poisson's ratio under undrained conditions,  $\nu_u$ ; density of the fluid in the reference state,  $\rho_0$ ; and Skempton's pore pressure coefficient,  $B$ . For relatively incompressible fluids such as oil and water,  $B$  is the ratio of solid volume change to the change in pore fluid volume (Segall 1985).  $B$  ranges between 0 and 1; for water-saturated soils  $B \approx 1$ ; for most rock types  $B$  ranges from 0.5 to 0.9 (Rice and Cleary 1976).

Consider a uniform, isotropic, fluid-infiltrated poroelastic half-space from which fluid with mass per unit solid volume  $\Delta v$  is uniformly extracted from pores of a small element. Because the resulting strain from fluid withdrawal is due to volume change only (Segall 1985)

$$\epsilon_{ij} = \frac{1}{3} \epsilon_{kk} \delta_{ij} \quad (1)$$

The constitutive equation for a poroelastic medium is a linear

<sup>1</sup>Ctr. for Computational Seismology, Earth Sci. Div., Berkeley Lab., 1 Cyclotron Rd., Berkeley, CA 94720.

<sup>2</sup>Earth Sci. Div., Berkeley Lab., 1 Cyclotron Rd., Berkeley, CA.

<sup>3</sup>Earth Sci. Div., Berkeley Lab., 1 Cyclotron Rd., Berkeley, CA.

Note. Discussion open until June 1, 1998. To extend the closing date one month, a written request must be filed with the ASCE Manager of Journals. The manuscript for this paper was submitted for review and possible publication on August 26, 1996. This paper is part of the *Journal of Geotechnical and Geoenvironmental Engineering*, Vol. 124, No. 1, January, 1998. ©ASCE, ISSN 1090-0241/98/0001-0029-0037/\$4.00 + \$.50 per page. Paper No. 14008.

relationship between solid matrix stress, pore fluid volume change, and the strains in the solid matrix

$$\epsilon_{ij} = \frac{\sigma_{ij}}{2\mu} - \frac{\nu_u}{2\mu(1 + \nu_u)} \sigma_{kk} \delta_{ij} + \frac{B\Delta v}{3\rho_0} \delta_{ij} \quad (2)$$

(Rice and Cleary 1976). Alternatively, this equation may be inverted and the stress may be written in terms of the strains

$$\sigma_{ij} = 2\mu\epsilon_{ij} + \lambda_u \epsilon_{kk} \delta_{ij} - \frac{BK_u \Delta v}{\rho_0} \delta_{ij} \quad (3)$$

where  $K_u$  signifies undrained bulk modulus

$$K_u = \frac{2\mu(1 + \nu_u)}{3(1 - 2\nu_u)} \quad (4)$$

and  $\lambda_u$  represents undrained Lamé constant (Segall 1985)

$$\lambda_u = \frac{2\mu\nu_u}{(1 - 2\nu_u)} \quad (5)$$

The volumetric strain in the solid matrix is proportional to the mean stress  $\sigma_{kk}$  and the change in pore fluid content  $\Delta v$ , from (2)

$$\epsilon_{kk} = \frac{\sigma_{kk}}{3K_u} + \frac{B\Delta v}{\rho_0} \quad (6)$$

The transformational strain resulting from a uniform change in fluid mass content  $\Delta v$  is (Segall 1985)

$$\epsilon_{kk}^T = \frac{B\Delta v}{\rho_0} \quad (7)$$

The free surface displacement is due to the propagation of stress within the elastic matrix of the half-space from the volume change source to the surface. For a point source, the surface displacement is proportional to the elastic response of a half-space acting at  $\mathbf{s}$ ,  $G_m(\mathbf{x}, \mathbf{s})$  (Segall 1985; Vasco et al. 1988)

$$u_n(\mathbf{x}) = CG_m(\mathbf{x}, \mathbf{s}) \quad (8)$$

where  $C$  = constant of proportionality. The constant of proportionality is given by the transformational strain of (7) times the volume change (Segall 1985)

$$C = \frac{B\Delta v}{\rho_0} dV \quad (9)$$

The total surface displacement due to a distribution of volume changes,  $\Delta v(\mathbf{s})$ , is given by a summation or integration over all elemental volume changes over the source volume  $V$

$$u_m(\mathbf{x}) = \frac{B}{\rho_0} \int_V \Delta v(\mathbf{s}) G_m(\mathbf{x}, \mathbf{s}) dV \quad (10)$$

where  $G_m(\mathbf{x}, \mathbf{s})$  = point source response function

$$G_m(\mathbf{x}, \mathbf{s}) = \frac{1}{3\pi} (\nu + 1) \frac{x_m - s_m}{S^3} \quad (11)$$

and  $S$  = distance from surface observation point,  $\mathbf{x} = (x_1, x_2, 0)$ , to source point,  $\mathbf{s} = (s_1, s_2, s_3)$

$$S = [(x_1 - s_1)^2 + (x_2 - s_2)^2 + s_3^2]^{1/2}$$

The  $i$ th component of surface tilt,  $t_i$ , is the gradient of the vertical displacement,  $u_3(\mathbf{x})$ , in the  $x_i$  direction

$$t_i(\mathbf{x}) = \frac{\partial u_3}{\partial x_i} = \frac{B}{\rho_0} \int_V \Delta v(\mathbf{s}) T_i(\mathbf{x}, \mathbf{s}) dV \quad (12)$$

where  $T_i(\mathbf{x}, \mathbf{s})$  is given by

$$T_i(\mathbf{x}, \mathbf{s}) = -\frac{1}{\pi} (\nu + 1) \frac{(x_i - s_i)(x_3 - s_3)}{S^5} \quad (13)$$

Note that (12) is a volume integral over an arbitrarily shaped body. An idealized fracture can be represented by taking one dimension to zero. In such a case, one dimension shrinks down to zero and the integral may be written in terms of a surface density. An alternative interpretation is that the fracture surface is surrounded by a flattened box that represents a boundary over which elastic strain is occurring.

## Inversion of Tilt Measurements

In considering the inversion of (12), that is, the inference of  $\Delta v(\mathbf{s})$  given a set of tilt data, the most important thing to note is the linear relationship between volume change in the subsurface and surface tilt. Thus, techniques from linear inverse theory and linear algebra may be utilized (Menke 1984; Parker 1994). The overall strategy is to convert the inverse problem into a linear system of equations that may be solved by a least-squares algorithm (Nobel and Daniel 1977).

We discretize the problem by subdividing the volume  $V$  into a finite number of nonoverlapping cells, say,  $N$  blocks. Each block may undergo a distinct volume change, say,  $\delta v_j$  for the  $j$ th cell. The individual tilt observed at  $\mathbf{x}$  due to the volume change  $\Delta v_j$  is an integral of the point source response function over the cell, where  $\Delta v_j$  is constant over the whole cell

$$t_i^j(\mathbf{x}) = \Delta v_j \int_{V_j} T_i(\mathbf{x}, \mathbf{s}) dV \quad (14)$$

Note that the integration volume is now  $V_j$ , the volume of the  $j$ th cell. The total tilt response is a sum over all  $N$  cells into which  $V$  has been divided

$$t_i(\mathbf{x}) = \sum_{j=1}^N t_i^j(\mathbf{x}) = \sum_{j=1}^N \Delta v_j \int_{V_j} T_i(\mathbf{x}, \mathbf{s}) dV = \sum_{j=1}^N \Delta v_j \Gamma_j(\mathbf{x}) \quad (15)$$

where  $\Gamma_j(\mathbf{x})$  represents integrated response of  $j$ th cell

$$\Gamma_j(\mathbf{x}) = \int_{V_j} T_i(\mathbf{x}, \mathbf{s}) dV \quad (16)$$

Given a set of  $M$  tilt observations, each of which is related to the distribution of volume change in the subsurface by an equation such as (15), a system of  $M$  equations in  $N$  unknowns may be constructed, which we write in matrix form as

$$\mathbf{t} = \mathbf{G}\mathbf{v} \quad (17)$$

where vector  $\mathbf{t}$  contains  $M$  tilt observations as components;  $\mathbf{G} = M \times N$  matrix whose components are given by (16); and  $\mathbf{v}$  = vector of  $N$  unknowns  $\Delta v_j$ ,  $j = 1, \dots, N$ .

One might attempt to solve the system of data equations [(17)] directly. For example, a common approach is to find the volume changes  $\mathbf{v}$  for which the sum of the square of the residuals

$$\mathbf{r}^T \mathbf{r} = (\mathbf{t} - \mathbf{G}\mathbf{v})^T (\mathbf{t} - \mathbf{G}\mathbf{v}) \quad (18)$$

is a minimum (Parker 1994). This often leads to a numerically unstable solution that is very sensitive to any error, be it numerical or observational. The more robust approach is to augment the data equations with some form of prior constraints on the solution, with prior assumptions restricting the range of possible volume change spatial distributions. One such assumption is that the volume change in the subsurface is simply connected. That is, if fluid is injected into or withdrawn out of a well penetrating the subsurface, we do not expect isolated volume changes that do not communicate with the well. This

may be phrased in terms of the roughness of the distribution of volume changes. In particular, we expect a smooth model, as measured by the spatial variations of the subsurface volume change. For example, the first horizontal difference of the volume change for the  $i$ -cell is

$$\delta v_i = v_i - v_{i+1} \quad (19)$$

while the second difference is

$$\delta_{v_i}^2 = 4v_i - v_{i+1} - v_{i-1} - v_{i+K} - v_{i-K} \quad (20)$$

where  $v_{i+1}$ ,  $v_{i-1}$ ,  $v_{i+K}$ , and  $v_{i-K}$  = adjacent cells in particular layer of blocks. One advantage of such a measure is that it is linear in the volume changes; thus, such constraints merely augment the linear system of equations [(17)] with more linear constraints. A measure of model roughness involving spatial differences such as (19) may be written in matrix form as (Menke 1984)

$$\mathbf{s} = \mathbf{D}\mathbf{v} \quad (21)$$

Hence, the sum of the squares of the components of the difference vector is

$$\mathbf{s}^T \mathbf{s} = (\mathbf{D}\mathbf{v})^T (\mathbf{D}\mathbf{v}) = \mathbf{v}^T \mathbf{L} \mathbf{v} \quad (22)$$

where  $\mathbf{L} = \mathbf{D}^T \mathbf{D}$ . Thus, a linear combination of data mis-fit and model roughness could be minimized as

$$P(\mathbf{v}) = (\mathbf{t} - \mathbf{G}\mathbf{v})^T (\mathbf{t} - \mathbf{G}\mathbf{v}) + W_s \mathbf{v}^T \mathbf{L} \mathbf{v} \quad (23)$$

where  $W_s$  = coefficient controlling relative importance of obtaining smooth model and fitting tilt observations. For large  $W_s$ , priority is given to obtaining a smooth model, while for small  $W_s$ , fitting the data is the prime objective. For  $W_s = 0$  we obtain the original least-squares problem given by (18). Minimizing the penalized mis-fit functional leads to the normal equations of linear least squares (Menke 1984), which may be solved directly. Note that the trade-off parameter  $W_s$  may be chosen arbitrarily. In the applications section, we briefly discuss one strategy for arriving at a value of  $W_s$ .

## APPLICATIONS

### Raymond Quarry Pump Test

The Raymond Quarry test site, in the foothills of the Sierra Nevada, serves as a natural laboratory for evaluating geophysical and hydrological techniques for mapping fractures (Cohen 1995). Because the major pathway for flow in many rock types is through fractures, it is important to develop techniques for characterizing flow and transport in fractures. Even if the geometry of a fracture is known, say, from intersections with various boreholes, the permeability in the fracture plane may vary by orders of magnitude. Therefore, it is essential that we develop techniques to estimate fracture flow properties.

Between March and May of 1992, a cluster of nine approximately 90 m deep boreholes were drilled at the Raymond field site (Cohen 1995). The wells are arranged in a rough V pattern, whose apex points north [Fig. 1(a)]. The wells on the western leg constitute the southwest (SW) series, while those on the eastern part are designated as southeast (SE). The spacing between wells along each arm of the V is roughly 7.5, 15, 30, and 60 m (Vasco et al. 1996). Driller's logs indicate that the granodiorite lies below approximately 8 m of soil and regolith. The tonalite may also intersect the wells at depth (Cohen 1995).

Results from geophysical and hydrological tests and logs indicate that the flow is confined to a few subhorizontal fracture zones (Karasaki et al. 1994). The current conceptual

model [Fig. 1(b)] consists of two dominant fracture zones: a shallow one between 25 and 40 m, and a deeper zone between 54 and 85 m in depth (Cohen 1995). The vertical black bars of this figure represent zones of low resistivity ( $<700 \text{ ohm} \cdot \text{m}$ ), and the circles locate measured flow zones. Furthermore, there are indications that there is a high degree of heterogeneity within the zones (Karasaki et al. 1994). These observations have been confirmed by crosswell seismic imaging (Vasco et al. 1996).

Surface tilt was proposed as one method for characterizing fractures and flow within fractures. To this end, Infraseismic Diagnostic Monitoring of Bakersfield, Calif., was contracted to deploy an array of tiltmeters and to monitor a series of fluid injection and withdrawal experiments. The proposed array consisted of 14 biaxial, high-gain tiltmeters in boreholes, each slightly deeper than 1 m. The instruments were laid out between August 8 and August 11, 1995, and the emplaced tiltmeters were allowed to settle before the start of production testing on August 14. During the interim, the instruments were continuously monitored in order to obtain the tidal and thermal background tilts prior to the well tests. An extended production test, of approximately 2 h duration, was conducted on the morning of August 15. It is that test which we shall analyze in detail. Following the extended test, several fluid injection tests were performed, each of varying duration.

Because the Earth's surface is continuously responding to temperature variations, pressure changes, and lunar and tidal forces, the surface tilt is a time-varying field. For shallow emplacements such as ours, the thermal response dominates, as shown in Fig. 2(a). In this figure, the north-south and east-west tilt series are shown for two of the 13 tiltmeters used. The experiment we shall discuss, pumping water from well 00, commenced slightly after 132 h. From Fig. 2(a), it is clear that the tilt variations due to thermal expansion and contraction are the dominate feature, obscuring the tilt variations due to the pump test. To remove the temperature response, a moving-average filter was applied to the tilt time series. However, because the frequency range of the pump test response and the temperature variations overlap, the filtering degraded the signal of interest. As the temperature variations the day preceding the pump test were similar to the temperature variations on the day of the pump test, another approach was attempted. From each tilt measurement made during the pump test, we simply subtracted the tilt observed exactly 24 h prior to that time. The resulting differential tilt is shown in Fig. 2(b) for the two tiltmeters in Fig. 2(a). The two vertical lines in this figure denote the beginning and the end of pumping from well 00. A measure of the success in removing the thermal effects is the preevent tilt variations. If all tilts unrelated to the test have been removed, the tilt should be zero prior to the start of pumping [denoted by the first vertical line in Fig. 2(b)]. For the most part, the tilt is zero prior to pumping; the principal exception was found at tiltmeter 14. We use the deviations of the prepumping tilt as a measure of error associated with the data from each tiltmeter.

Beginning shortly after noon on August 15, water was pumped from well 00 at a rate of 6 gal./min for 2 h, 7 min. The total volume pumped from well 00 was estimated to be 3,400 L. The pumping was concentrated in a packed off interval in the well between 29.6 m and 32.4 m in depth. The packer placement isolated that portion of the well intersecting the uppermost fracture zone (Fig. 1).

To infer the volume change in the subsurface compatible with the observed tilt, we first constructed a representation of the fracture zone. From the well logs, we observed that no one fracture may be singled out as a dominant conducting feature (Cohen 1995). Rather, an irregular zone of fractures up to 5 m in width appears to control the flow. Furthermore, this zone

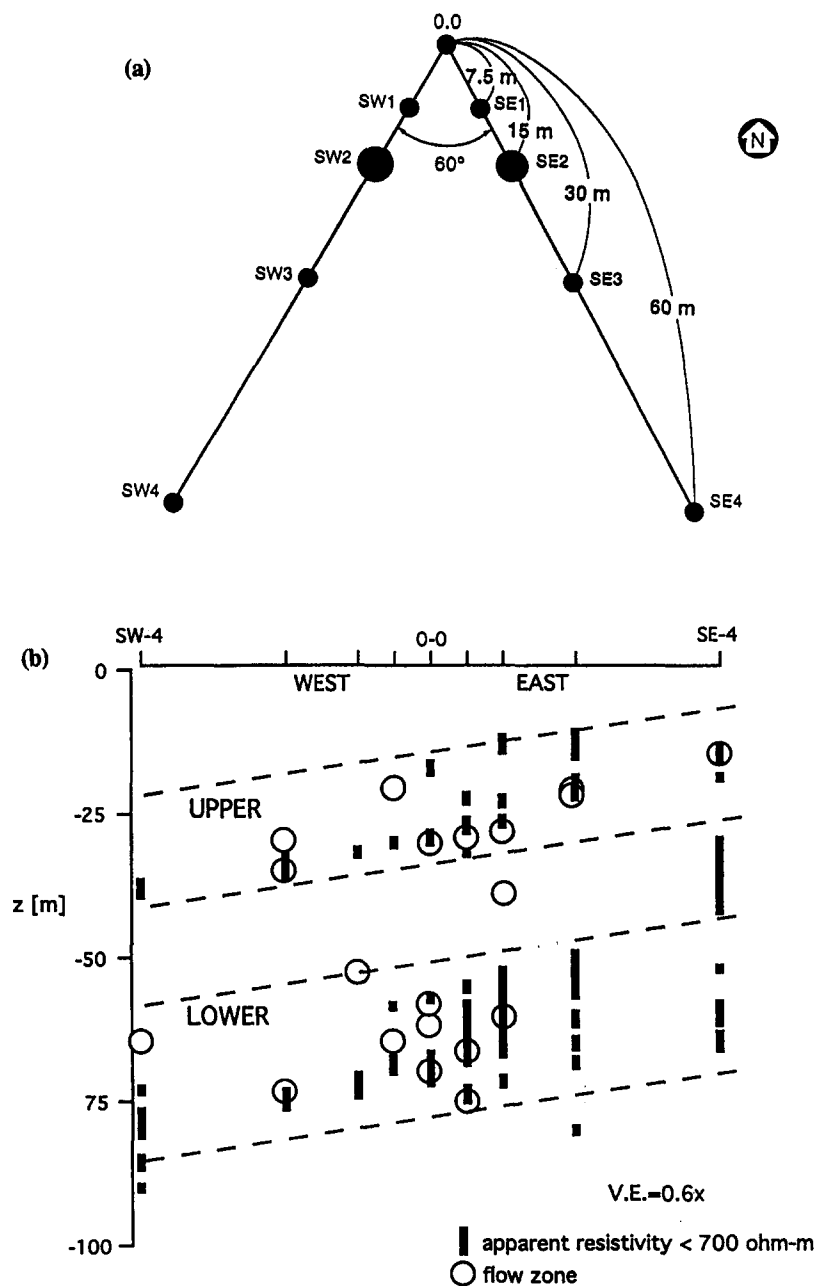


**FIG. 1. Raymond Test Facility: (a) Location Map Denoting Placement of Boreholes; (b) Conceptual Model of Important Hydrological Features**

appears to dip to the west, as shown in Fig. 1. Therefore, to allow for the westward dip, we represented the fracture zone as three distinct layers, each 3 m thick. The top of the layers was at a depth of 20 m, and the bottom lay at 29 m. Each layer was subdivided into a  $20 \times 20$  grid of cells; the lateral dimension of each block was 5 m, for a total of 1,200 grid blocks. The granite was modeled as a homogeneous elastic half-space with a Poisson's ratio of 0.25.

In addition to fitting the data, we required a somewhat smooth model by including a penalty term in the inversion, as in (23). As mentioned previously, the weighting coefficient  $W_r$  may be chosen arbitrarily. We estimated  $W_r$  by constructing a trade-off curve, a standard approach in geophysical inverse problems (Menke 1984). Specifically, a number of inversions were conducted for systematically varying values of  $W_r$ . After each inversion, we computed the model roughness, as measured by the second differences between cells, and data fit generated by the estimated model. These values were plotted as a curve parameterized by  $W_r$  (Fig. 3). We choose  $W_r$  to

correspond to the bend or knee in the parameterized curve, the point nearest the origin. For  $W_r$  values greater than this, the data misfit grows large rapidly; for smaller values, the roughness increases dramatically.

The tilt data (Fig. 2) are of such high quality (high signal to noise) that it was possible to invert for cumulative fractional volume change as a function of time (Fig. 4). The arrows in this figure represent the tilt data used in the respective inversions. The circles denote tiltmeter locations, and the triangles are located at well 00 (topmost) and well SE-1. The diameters of the circles are proportional to the estimated errors of the observations, while the lengths of the arrows are proportional to the observed tilt magnitude. In this experiment, water was pumped from well 00, the uppermost triangle. As mentioned earlier, three layers were used in the model in order to represent the dipping nature of the fracture zone and the fact that no single fracture appears to define the fracture zone. The vertical resolution provided by surface displacement data is rather poor (Vasco et al. 1988), and it is not possible to control trade-

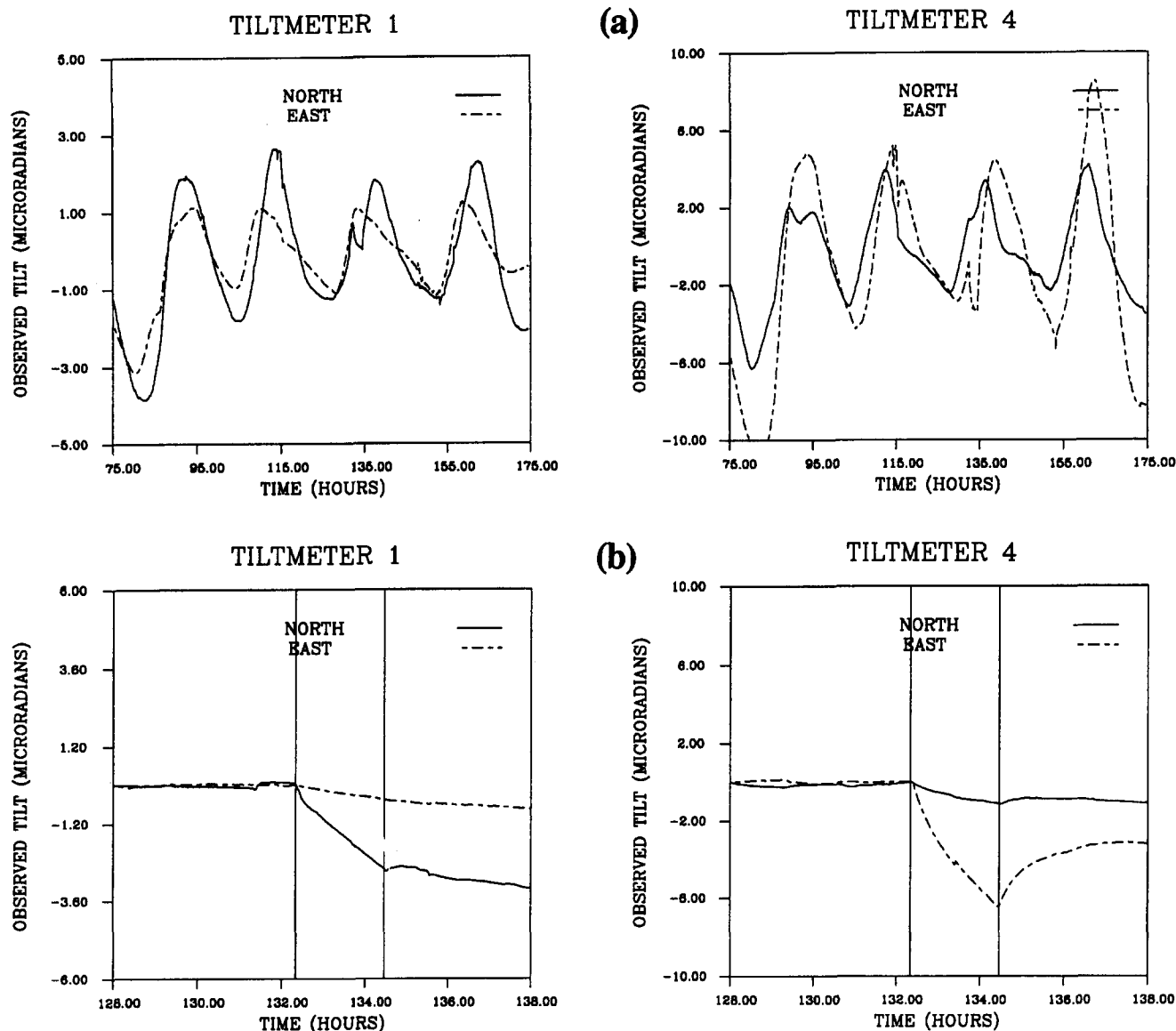


FIG. 2. Diagram of: (a) Raw Tilt Data from Raymond Production Test, Portraying Tilt As Function of Time for Two of 13 Tiltmeters Considered; (b) Tiltmeter Data with Estimated Background Variations Removed

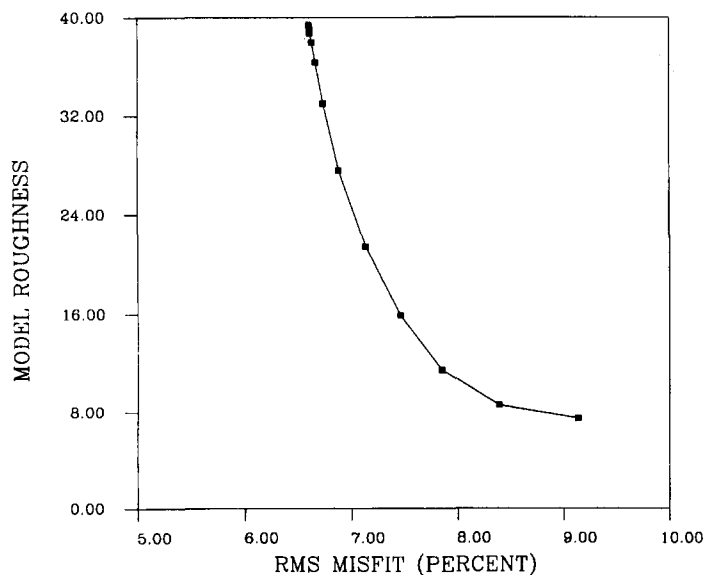


FIG. 3. Trade-Off Curve Portraying Variation of RMS Misfit and Model Roughness, Parameterized by Coefficient  $W_s$

offs between the volume change in adjacent layers. Therefore, in this figure we show the vertically summed fractional volume change in the three layers. The fractional volume change in this figure has been scaled (multiplied) by  $10^{-5}$ . The time varying volume decreases in the fracture zone appear to be largest to the south and west of the pumping well 00 (Fig. 4). The zone of volume decrease is elongated in a north-south direction. This agrees with a qualitative analysis of some 3,600 pressure transient curves for 31 well tests conducted between various SE and SW wells (Fig. 1), as described in the work by Cook (1995). A stronger hydraulic connectivity was found in the north-south direction than was observed in the east-west direction. The total set of predictions for all tiltmeters for all six intervals are shown in Fig. 5, plotted against the tilts that we observed. The predicted tilts agree quite well with the observed data. The several data values that have large associated errors are from tiltmeter 14, which was quite noisy.

#### Los Banos Grout Injection

The injection of grout into fluid conducting features can produce a barrier to contaminant transport. Therefore, grout injection is a potential remediation tool that may hydrologi-

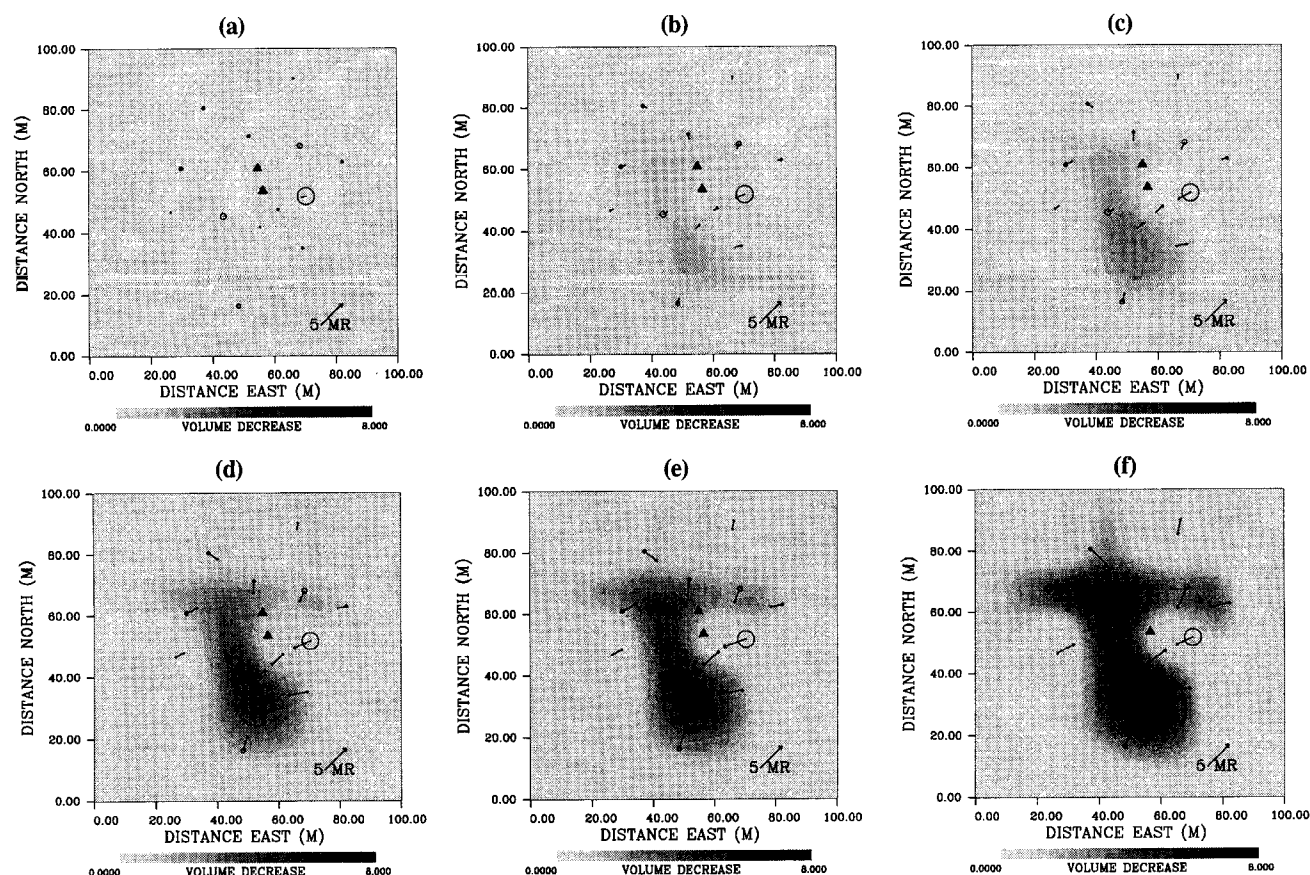


FIG. 4. Cumulative Fractional Volume Change for Six Successive Time Intervals [Fractional Volume Change Is Denoted by Gray Scale and Has Been Scaled (Multiplied) by  $10^{-5}$ ]: (a) 3 min; (b) 12 min; (c) 21 min; (d) 42 min; (e) 60 min; (f) 120 min

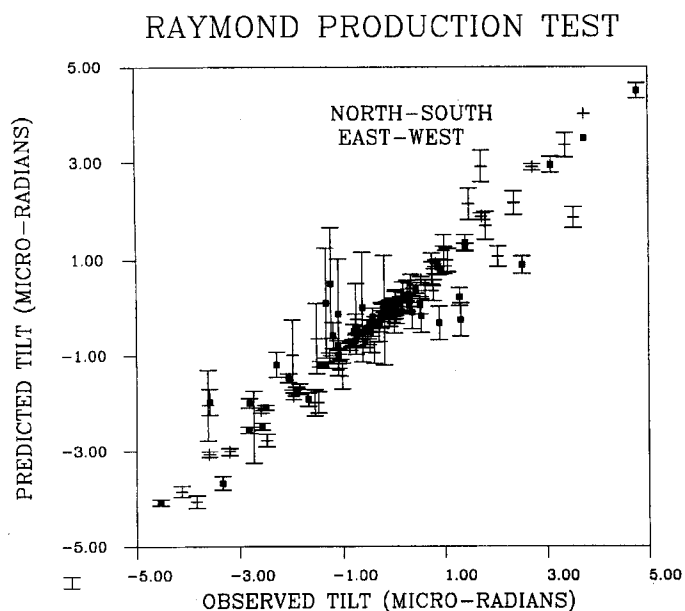


FIG. 5. Observed versus Predicted Tilt for All Data from Six Time Intervals Shown in Fig. 4 (Error Bars of One Estimated Standard Error Are Also Shown)

cally isolate pollutants in the subsurface. As a demonstration of this technology, Berkeley National Laboratory, Berkeley, Calif., in collaboration with Bechtel Engineering, conducted a field experiment in the winter of 1995. In this experiment, grout was injected into a porous gravel at a shallow depth of 3–4 m. It was hoped that tiltmeters could provide one means of monitoring the injection. There were limitations in the experiment, such as the existence of a nearby cliff face, settling

of the instruments, a small tilt signal due to large air-filled pores in the gravel medium, and migration of the grout up the injection borehole. These difficulties proved a significant challenge to the analysis, though we were able to extract information on the overall geometry of the grout migration.

As part of this first-level field demonstration, eight sensitive tiltmeters were deployed around two injection wells. The tiltmeters were placed in shallow holes, less than 1 m deep, and were surrounded by packed sand. In an effort to estimate background noise and trends, tilt observations were obtained for several hours of ground motion on the day prior to the test. Such data provide an important measure of the trends in surface tilt due to environmental factors such as tiltmeter settling, barometric pressure changes, temperature, and so on. It rained prior and during the injection events, and while the cloud cover reduced the thermal variations, it introduced settling and possible swelling in the ground and in the sand pack surrounding each instrument. Tilt data were acquired for two sets of experiments: the injection of colloidal silica (CS) grout and the injection of polysilica grout. Between the two injection episodes, the tiltmeters were reconfigured. We shall examine the tilting induced by the injection of CS.

Fig. 6 displays the north-south and east-west components for four of the eight tiltmeters. The vertical lines in the figure denote the start of individual injection intervals. For tiltmeters 1 and 2, there are apparent correlations with tilt changes and the start of injection events. Thus, we were able to resolve individual injection events even though the current configuration of instruments was less than optimal. Note the variations of signal to noise in the time series from each tiltmeter. In particular, tiltmeters 4 and 6, which were close to a cliff face, are extremely noisy. To some extent, the presence of the cliff face violates the half-space assumption. However, the cliff face was remote enough relative to the depth of the injection (twice

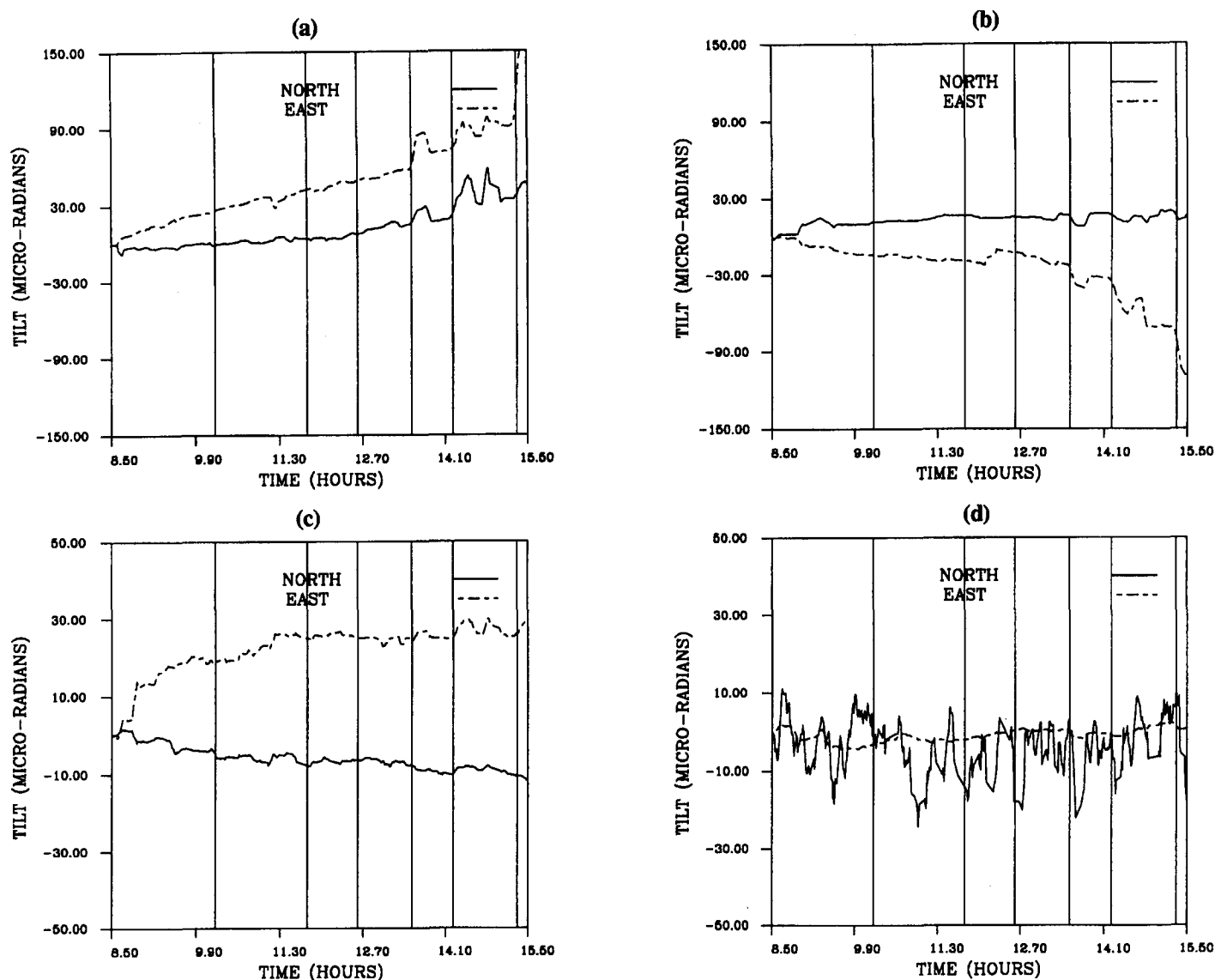


FIG. 6. Surface Tilts Associated with Injection of Colloidal Silica (CS) (Individual Injection Events Are Denoted by Vertical Lines): (a) Tiltmeter TC-1; (b) Tiltmeter TC-2; (c) Tiltmeter TC-3; (d) Tiltmeter TC-4

as far as the depth) that its influence was much smaller than the tiltmeter noise level. Because the instruments only began recording the day before the experiment, we were unable to estimate the background variations as in the Raymond experiment discussed before, mainly due to the transient nature of tiltmeter settling, a serious drawback. As a rough estimate of the background variation, a linear trend was subtracted from the components of tilt based upon the trend just prior to the experiment, as well as from the linear trends observed in the previous day's noise measurements. Differential tilt was calculated by subtracting the tilt at each station prior to the injection (10:00 a.m.) from the subsequent tilt time series.

In this analysis, we consider three overlapping time intervals: 10:00 a.m.–12:00 a.m., 10:00 a.m.–14:00 a.m., and 10:00 a.m.–15:00 a.m. (Fig. 7). In Fig. 7, the tilt vectors are shown in map view along with their respective uncertainties. The length and direction of the arrows denote the extent and direction of tilt. The open circles denote the uncertainty associated with the change in surface tilt. The uncertainties are greatest for tiltmeters 4 and 6, which are the two western most instruments, nearest the cliff face. In fact, for these meters the uncertainties (denoted by the circles) always exceed the observed tilt. The tiltmeters that experienced the most tilt are adjacent to the two injection wells (denoted by the black dots).

The tilt points away from the injection wells and begins to exceed the estimated noise level after about 12:00 a.m. The other instruments have not undergone significant tilting relative to the background noise.

We wish to determine the cumulative volume change that occurred in the subsurface within these time intervals. Specifically, we seek the distribution of effective volume displacement in the subsurface due to the cumulative grout injection for these time periods and for both wells. The analysis is based upon techniques developed for estimating volume change in a poroelastic medium discussed in the Methodology section. In this particular case, the fluid infiltrating the solid matrix was air, which differs from the injected fluid, which is grout. If the grout enters a void, due to the extreme compressibility of air, there will be little or no resulting surface displacement. Therefore, the volume changes are effective because there are indications that the formation was extremely porous and large voids were present. The parameters describing the relationship between the injected volume of grout and the effective volume change in the elastic matrix are given in (12), with the ratio of Skempton's pore pressure coefficient to the density of the fluid:  $B/\rho$ . Because we had no laboratory data constraining this ratio, we chose  $B/\rho$  such that the observed surface tilt from a point source agreed with the total injected volume (1,437 L).



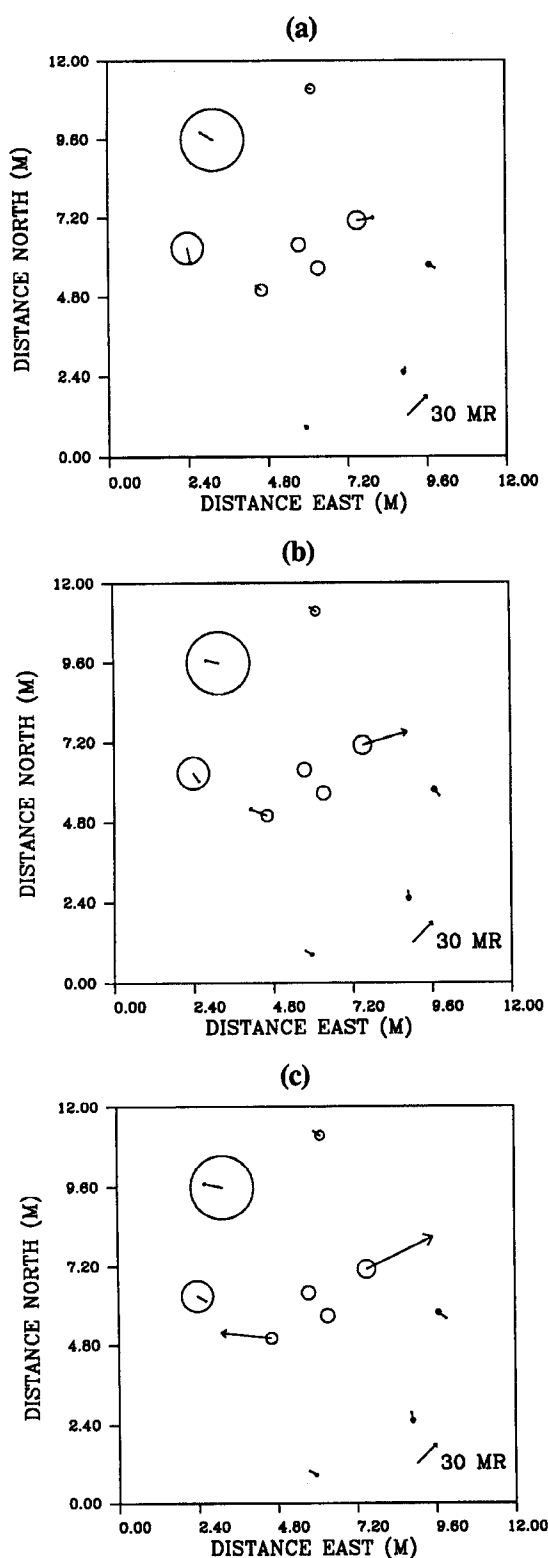


**FIG. 7. Changes in Surface Tilt for Three Cumulative Time Intervals—12:00 a.m.–10:00 a.m., 14:00 a.m.–10:00 a.m., and 15:00 a.m.–10:00 a.m. (Empty Circles Denote Location of Two Injection Wells): (a) Observed Tilt (12H)–Tilt (10H); (b) Observed Tilt (14H)–Tilt (10H); (c) Observed Tilt (15H)–Tilt (10H)**

Thus, it was not possible to independently check the injected volume against the predicted injected volume. The techniques from geophysical inverse theory described before allow us to infer the effective distribution of grout injected over a given time interval.

Though the injection occurred through ports at several dis-

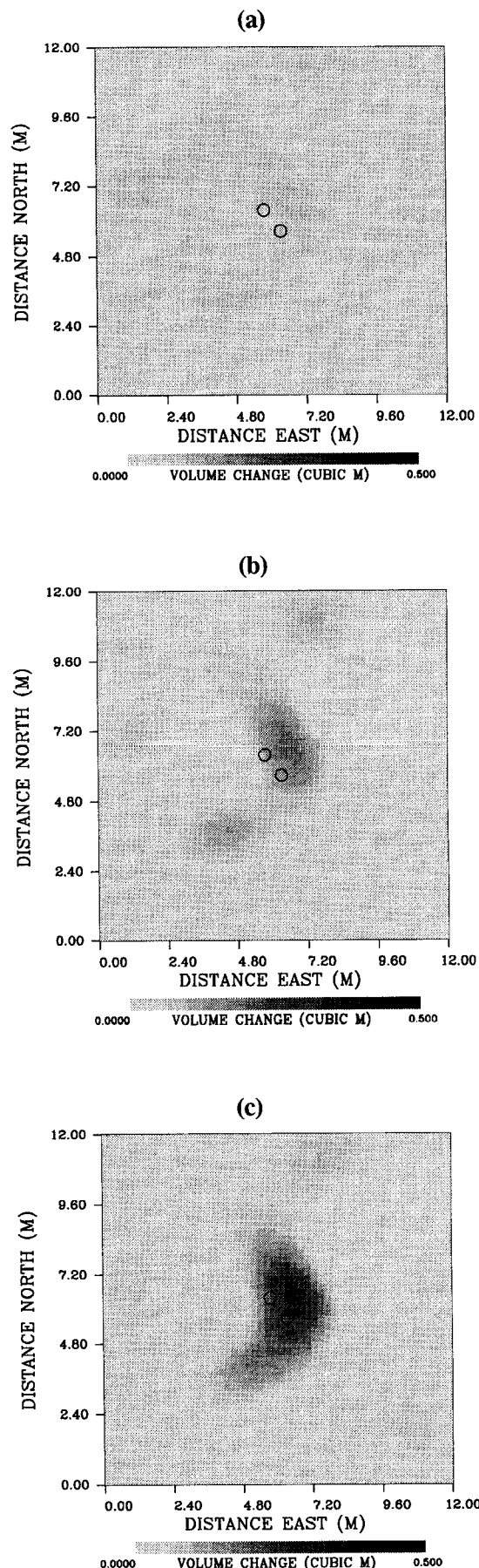


**FIG. 8. Inferred Volume Change in Depth Interval 3.0–4.3 m [Gray Scale Denotes Effective Volume Change ( $m^3$ ) in Layer over Successive Time Intervals: (a) Tilt (12H)–Tilt (10H); (b) Tilt (14H)–Tilt (10H); (c) Tilt (15H)–Tilt (10H)]**



crete depths, the surface displacement data do not have sufficient vertical resolution to distinguish the individual events. Therefore, a composite layer 3–4.3 m in depth was used to model the cumulative grout injection from the two wells. The effective volume changes estimated through inversion of the tilt data are shown in Fig. 8. For the time interval 12:00 a.m.–10:00 a.m., the tilt signal does not exceed the noise level. Therefore, the injected volume is quite small and is distributed in several places in the 3–4.3 m layer. For the time interval 14:00 a.m.–10:00 a.m., we begin to resolve significant injected volume. The concentration of material is below and to the northeast of the two wells. The cumulative injected volume for a slightly greater time interval, 15:00 a.m.–10:00 a.m., is larger still. Again the injected volume appears to have migrated to the northeast, with some material extending to the southwest.

After the injection experiment and the analysis of all the available data, the gravel surrounding the injection was excavated and the distribution of the grout was mapped. This provided a check on our inversion results and our modeling effort. While it was found that the CS grout created fairly uniform plumes, there was some concentration of the grout in particular zones. In particular, a tail of grout trending southwest from the pair of wells was observed in the excavated mass in agreement with the inversion results (Fig. 8). Unfortunately, some grout was also observed to have traveled vertically, parallel to the well bore, and to have spread out at a shallower depth, approximately 1 m below the surface. These additional volume changes were not accounted for by our single layer inversion, and the tilt data are not of high enough quality to warrant such detailed modeling. If the data were less contaminated and the station distribution denser, the volume changes adjacent to the entire borehole could have been determined by the tiltmeter measurements, included as unknowns in the inversion.

## ANALYSIS AND CONCLUSIONS

We have described a methodology for using tiltmeter data to infer subsurface fluid flow. Our analysis is based upon volume changes in a homogeneous poroelastic half-space. Several improvements or extensions are possible, including developing a point source response function for a layer over a half-space to account for the soil layer. More general numerically intensive approaches are also available, such as finite-difference and finite-element techniques (Smith 1982), with a corresponding increase in computation time. The additional complexity necessitates more complete knowledge of the subsurface, such as a distribution of Poisson's ratio, and more effort to set up the model.

This preliminary work suggests that tilt measurements may be used to monitor subsurface volume changes. At the Raymond test facility, tilt measurements provided constraints on the fluid flow in a fracture zone. The results agree with the analysis of some 3,600 transient pressure curves gathered from nine packed-off wells at the facility. At the Los Banos site, in spite of the significant void space in the material and the inexperience with the tiltmeter instrumentation, we are able to measure tilt associated with individual grout injection events. A constrained inversion of the tilt data allowed us to extract an estimate of the deeper component of volume change. However, the elaboration of the experiment and the analysis point to aspects that must be considered in tiltmeter monitoring. In more favorable circumstances, more competent host rock, better placement of the tiltmeters, and extended monitoring before and after the injections, the constraints on the grout placement would be even stronger. This conclusion is strengthened by the fact that oil-field hydrofracturing experiments, for fracturing at hundreds of meters to more than 1,000 m, are routinely monitored by tiltmeters.

## ACKNOWLEDGMENTS

This work was carried out under U.S. Department of Energy Contract No. DE-AC03-76SF00098, for the director, Office of Civilian Radioactive Waste Management, Office of External Relations, administered by the Nevada Operations Office in cooperation with the AECL of Canada and the U.S. Geological Survey. All computations were carried out at the Center for Computational Seismology of the Lawrence Berkeley Laboratory.

## APPENDIX. REFERENCES

- Aki, K., and Richards, P. G. (1980). *Quantitative seismology*. Freeman and Sons.
- Biot, M. A. (1941). "General theory of three-dimensional consolidation." *J. Appl. Phys.*, 12, 155–164.
- Bruno, M. S., and Bilak, R. A. (1994). "Cost-effective monitoring of injected steam migration using surface deformation analysis." *Proc., SPE Western Regional Meeting, SPE 27888*, 397–412.
- Bruno, M. S., and Nakagawa, F. M. (1991). "Pore pressure influence on tensile fracture propagation in sedimentary rock." *Int. J. Rock Mech. and Mining Sci. & Geomech. Abstracts*, 28, 261–273.
- Chilingarian, G. V., Donaldson, E. C., and Yen, T. T. (1995). *Subsidence of petroleum reservoirs due to fluid withdrawal*. Elsevier Applied Science, New York, N.Y.
- Cohen, A. J. B. (1995). "Hydrogeologic characterization of fractured rock formations." *Rep. LBL-31842*, Ernest Orlando Lawrence Berkeley Nat. Lab., Berkeley, Calif.
- Cook, P. (1995). "Analysis of interwell hydraulic connectivity in fractured granite," MS thesis, Univ. of California at Berkeley.
- Davis, P. M. (1983). "Surface deformation associated with a dipping hydrofracture." *J. Geophys. Res.*, 88, 5826–5834.
- Du, Y., Aydin, A., and Murdoch, L. (1993). "Incremental growth of a shallow hydraulic fracture at a waste remediation site, Oakbrook, Illinois from inversion of elevation changes." *Int. J. Rock Mech. and Mining Sci. & Geomech. Abstracts*, 30, 1273–1279.
- Dusseault, M. B., Bilak, R. A., and Rothenburg, L. (1993). "Inversion of surface displacements to monitor in-situ processes." *Int. J. Rock Mech. and Mining Sci. & Geomech. Abstracts*, 30, 1219–1222.
- Evans, K. F., Holzhausen, G. R., and Wood, M. D. (1982). "The geometry of a large-scale nitrogen gas hydraulic formed in Devonian shale: An example of fracture mapping using tiltmeters." *SPE J.*, 22, 755–763.
- Karasaki, K., Freifeld, B., and Davison, C. (1994). "A characterization study of fractured rock." *Proc., 5th Int. High Level Radio. Waste Mgmt. Conf.*
- Melan, E. (1932). "Der spannungszustand der durch eine einzelkraft im innern beanspruchten halbscheibe." *Angew. Math. Mech.*, 12, 343–346 (in German).
- Menke, W. (1984). *Geophysical data analysis: Discrete inverse theory*. Academic Press, Orlando, Fla.
- Nobel, B., and Daniel, J. (1977). *Applied linear algebra*. Prentice-Hall, Inc., Englewood Cliffs, N.J.
- Palmer, I. D. (1990). "Uplifts and tilts at Earth's surface induced by pressure transients from hydraulic fractures." *SPE Production Engrg.*, 5, 324–332.
- Parker, R. L. (1994). *Geophysical inverse theory*. Princeton University Press, Princeton, N.J.
- Pollard, D. D., and Holzhausen, G. (1979). "On the mechanical interaction between a fluid-filled fracture and the Earth's surface." *Tectonophys.*, 53, 27–57.
- Rice, J. R., and Cleary, M. C. (1976). "Some basic stress diffusion solutions for fluid-saturated elastic porous media with compressible constituents." *Rev. Geophys.*, 14, 227–241.
- Segall, P. (1985). "Stress and subsidence resulting from subsurface fluid withdrawal in the epicentral region of the 1983 Coalinga earthquake." *J. Geophys. Res.*, 90, 6801–6816.
- Smith, I. M. (1982). *Programming the finite element method with applications to geomechanics*. John Wiley & Sons, Inc., New York, N.Y.
- Vasco, D. W., Johnson, L. R., and Goldstein, N. E. (1988). "Using surface displacement and strain observations to determine deformation at depth, with an application to Long Valley Caldera, California." *J. Geophys. Res.*, 93, 3232–3242.
- Vasco, D. W., Peterson, J. E., and Majer, E. L. (1996). "A simultaneous inversion of seismic travel times and amplitudes for velocity and attenuation." *Geophys.*, 61, 1738–1757.
- Vasco, D. W., Smith, R. B., and Taylor, C. L. (1990). "Inversion for sources of crustal deformation and gravity change at the Yellowstone Caldera." *J. Geophys. Res.*, 95, 19839–19856.
- Volterra, V. (1907). "Sur l'équilibre des corps élastiques multiplément connexes." *Ann. Sci. Ecole Norm. Supér. Paris*, 24, 401–517 (in French).